DOI: 10.3969/j.issn.1673-3185.2017.03.016 **http**: // english.ship-research.com

Translated from: YAO X L, MENG L W, NIU X L. LQR pitch control strategy of AUVs based on the optimum of sailing resistance [J]. Chinese Journal of Ship Research, 2017, 12(3): 111-119.

LQR pitch control strategy of AUVs based on the optimum of sailing resistance

YAO Xuliang, *MENG Lingwei*, *NIU Xiaoli*

College of Automation, Harbin Engineering University, Harbin 150001, China

Abstract: When an Autonomous Underwater Vehicle (AUV) sails near the surface of the sea, it will inevitably be subjected to wave disturbance. The heave and pitch motion caused by wave disturbance not only affects the navigation attitude of the AUV, but also leads to an increase in sailing resistance. As such, its energy consumption is increased. In this paper, the six degrees of freedom model of AUVs is established and linearized in order to achieve the weighted optimization of the sailing attitude and the resistance of the AUVs. The drag force model of the AUV is derived using the theory of potential flow. The Q matrix and R matrix are determined in the controller based on research into the drag force model. The Linear Quadratic Regulator (LQR) controller of the AUV is designed using the drag force model as the performance index. The simulation results show that after adding the LQR controller, the effects of reducing heave motion and pitch motion are 46.64% and 77.62% respectively, and the increased resistance caused by the pitch motion is reduced to 1/6 of its original value. The results show that the multiple optimum of attitude and sailing resistance is realized, the energy consumption is decreased and the endurance of the AUV is increased.

Key words: optimum of sailing resistance; LQR control; pitch stabilization; potential theory

CLC number: U664.82

0 Introduction

When an Autonomous Underwater Vehicle (AUV) performs tasks, energy consumption is the main factor affecting its sailing capacity, and the energy consumption depends mainly on the sailing resistance. When AUV sails near the water surface, the pitch motion induced by waves will lead to an increase in the sailing resistance. AUV carries a limited amount of energy, and an increase in resistance can lead to a decrease in endurance.

The International Maritime Organization (IMO) has proposed a new ship Energy Efficiency Design Index (EEDI) [1], which requires considering the energy saving problem of AUV in the design of AUV pitch stabilization controller. The control strategy not only pursues the minimum motion amplitude, but also considers the optimization of drive device energy and added resistance by pitch[2]. Based on the radiation energy theory, the roll amplitude of ship will increase the sailing resistance of the ship. Therefore, in the design of fin controller for ship roll stabilization, the added resistance by roll should be taken into account[3]. However, in the design of AUV pitch controller, the added resistance by pitch is hardly involved. Therefore, a drag force model of AUV is needed and will be used as the performance index of the AUV pitch control.

With the increasingly wide application of AUV, the research on AUV is deeper. The C-SCOUT AUV is used for the sampling of marine geography, and its dynamic model analyzes its external force and hydrodynamic force of control surface[4]. The Dolphin MK II semi-submersible AUV has been developed by

Received: 2016 - 11 - 07

Supported by: National Natural Science Foundation of China (51279039)

Author(s): YAO Xuliang, male, born in 1969, Ph.D., professor. Research interest: ship electric propulsion and advanced control theory. Corresponding author, E-mail: yao_1126@163.com

MENG Lingwei, male, born in 1987, Ph.D. candidate. Research interest: ship motion control. E-mail: menglingweiheu@msn.com

University of British Columbia, and by experiments, the quarter model was used to study the hydrodynamic forces of the overall AUV and control surface[5]. In view of the fact that the AUV is semi-submersible AUV, it will work near the water surface and be disturbed by wave force, so it is necessary to design a pitch controller so as to maintain a stable sailing attitude.

Ding[6] designed the LQR controller for the approach landing problem of aircraft, and solved the coordination problem of multiple control loops. Li et al. [7] designed the longitudinal attitude control law for flying-wing UAV using an augmented LQR method, which introduced the system output error and the disturbance signal by external constant gust into the performance index function. Duan[8] used the robust servo LQR controller for the pitch velocity loop of UAV. Bhushan et al.[9] analyzed the weight matrix of LQR control method based on genetic algorithm, and believed that the performance index based on genetic algorithm was more stable. Häusler et al.[10] added the performance index of energy optimization in the collision-free path planning of AUV. Liang et al.[11] analyzed the energy optimization of AUV in the case of external disturbances. Petrich et al.[12] analyzed the simplification of vertical axis of AUV. Wang et al.[13] analyzed the energy optimization problem of pitch stabilization at zero velocity, but did not propose the performance index of sailing resistance. Xu et al.[14] carried out energy optimization of the bow control of AUV and reduced the fluctuation of the yaw velocity. Chyba et al.[15] conducted energy optimization of the control method for AUV sailing between two points. Sarkar et al.[16] designed a sliding mode control method based on energy optimization, and achieved good results. In designing submersible vehicles, Li et al.[17] calculated the sailing resistance of submersible vehicles.

We can see that in previous studies, study on the sailing resistance is often involved in the process of hull design, and the sailing resistance is reduced by optimizing the molded lines, but study on the added sailing resistance caused by the pitch motion is few. In fact, the pitch motion of AUV will lead to the increase of the sailing resistance, and the swing of control surface will also increase the sailing resistance. The sailing resistance and pitch motion as well as control surface swing were positively correlated, namely, the more intense the pitch motion is, the more the sailing resistance increases, and the greater the control surface swings, the more the sailing resistance increases. However, the greater the swing amplitude of the control surface is, the more obvious the effect of pitch stabilization is. Therefore, in controlling the pitch motion of AUV, the added resistance by pitch and control surface should be both taken into account, so that the two can compromise to make the sailing resistance of AUV minimum, and then the energy consumption of propulsion will be reduced.

To achieve this goal, firstly, we need to study the relationship between the sailing resistance and the AUV attitude, and establish the mathematical model between the sailing resistance and the sailing attitude; secondly, the drag force model of the control surface also needs to be considered. In the design of the controller, the two should be considered jointly as a performance index so as to minimize the sailing resistance in the control process.

In this paper, we will take Dolphin MK II as the object of study to investigate its pitch control strategy. First of all, the drag force model of AUV will be established to quantitatively analyze the relationship between pitch attitude and sailing resistance. Secondly, the influence of control surface swing on added sailing resistance will be analyzed. Finally, the added resistance by pitch and the added resistance by control surface will be considered together, and by using it as a performance index, the pitch attitude controller of AUV is designed. A LQR controller is designed to combine the added resistance by pitch and the added resistance by control surface, so as to achieve the optimal sailing attitude resistance.

1 Near surface robot model

When an AUV sails near the water surface, it will be subjected to the wave disturbances, resulting in pitch motion and increase of the sailing resistance. Fig. 1 is the structure diagram of an AUV. In this paper, the Canadian Dolphin MK II AUV was used as a model to establish the nonlinear model and simulate the wave force/moment. In order to control the sailing attitude of AUV, the six-degree-of-freedom (6-DOF) nonlinear model of AUV was firstly established, and in order to facilitate the design of LQR controller, it was linearized in this paper. The control surface is the driving device of pitch stabilization, and the NACA0025 surface was adopted as the control surface. The hydrodynamic model of the control surface was established.

In the analysis of the force of AUV, we can regard AUV as a rigid body with uniform mass distribution.

According to Newton's law and the related knowledge of fluid mechanics, the 6-DOF equation of motion of AUV near the water surface was obtained. The parameters of Dolphin MK II AUV are shown in Table 1.

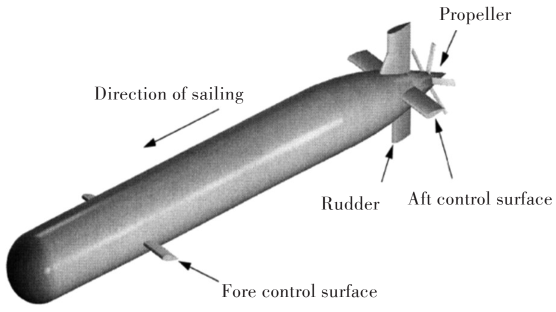

Fig.1 The structure of AUV

Table 1 Parameters of AUV

Total length /m	Mass/kg	Diameter /m	Tail length /m	Displacement /kg	Maximum sailing velocity/kn
8.534	4 300	1	2.35	4 600	18

From the dynamics knowledge, we know that the dynamic model of AUV is as follows:

$$\boldsymbol{M}_{\mathrm{rb}}\frac{\partial}{\partial t}\boldsymbol{v}+\boldsymbol{C}_{\mathrm{rb}}(v)\boldsymbol{v}=\boldsymbol{\tau}_{\mathrm{rb}} \tag{1}$$

where $\boldsymbol{M}_{\mathrm{rb}}$ is mass matrix; $\boldsymbol{C}_{\mathrm{rb}}(v)$ is the Coriolis matrix; $\boldsymbol{\tau}_{\mathrm{rb}}$ is the external force/external moment on AUV; $\boldsymbol{v}$ is the velocity matrix of AUV.

Generally, $\boldsymbol{\tau}_{\mathrm{rb}}$ is composed of three parts, i.e.

$$\boldsymbol{\tau}_{\mathrm{rb}}=\boldsymbol{\tau}_{\mathrm{h}}+\boldsymbol{\tau}_{\mathrm{w}}+\boldsymbol{\tau}_{\mathrm{c}} \tag{2}$$

where $\boldsymbol{\tau}_{\mathrm{h}}$ is hydrodynamic force/moment; $\boldsymbol{\tau}_{\mathrm{c}}$ is the control force/moment; $\boldsymbol{\tau}_{\mathrm{w}}$ is wave force/moment.

The hydrodynamic force and hydrodynamic moment acting on the AUV are

$$\boldsymbol{\tau}_{\mathrm{h}}=-\boldsymbol{M}_{\mathrm{A}}\dot{\boldsymbol{v}}-\boldsymbol{C}_{\mathrm{A}}\boldsymbol{v}-\boldsymbol{D}\boldsymbol{v}+\boldsymbol{\tau}_{\mathrm{bg}} \tag{3}$$

where $\boldsymbol{M}_{\mathrm{A}}$ is the added mass matrix; $\boldsymbol{C}_{\mathrm{A}}$ is the added Coriolis matrix; $\boldsymbol{\tau}_{\mathrm{bg}}$ is the restoring force/moment; $\dot{\boldsymbol{v}}$ is the acceleration matrix; $\boldsymbol{D}$ is the damping matrix.

The control force/moment produced by the AUV can be expressed as

$$\boldsymbol{\tau}_{\mathrm{c}}=\boldsymbol{B}\boldsymbol{u} \tag{4}$$

where $\boldsymbol{B}$ is the control matrix, and $\boldsymbol{u}$ is the control vector.

Thus, the matrix form of the AUV dynamic model can be obtained as

$$(\boldsymbol{M}_{\mathrm{rb}}+\boldsymbol{M}_{\mathrm{A}})\dot{\boldsymbol{v}}+(\boldsymbol{C}_{\mathrm{rb}}+\boldsymbol{C}_{\mathrm{A}}+\boldsymbol{D})\boldsymbol{v}=\boldsymbol{\tau}_{\mathrm{bg}}+\boldsymbol{\tau}_{\mathrm{w}}+\boldsymbol{B}\boldsymbol{u} \tag{5}$$

2 Simulation of wave force/moment

When the AUV sails near the water surface, it is subjected to ocean environmental disturbances such as waves and ocean current, which are uncertain and stochastic. Wherein, wave disturbance is the main factor causing AUV sway. In designing the AUV attitude controller, it is necessary to estimate the disturbing force/moment of the AUV when it sails near the water surface. In order to determine the force/moment of waves on AUV, the wave force must be simulated and calculated.

The wave force/moment of heave and pitch near the water surface were simulated by linear superposition method. Firstly, the spectral form of waves was selected, and the ITTC single parameter spectrum was selected in this paper. Then, the discrete method was used to obtain the harmonic amplitude of the waves according to the discrete wave spectrum. The initial phase angle was random number which can be given according to the random function. After each harmonic and initial phase angle were determined, the harmonics were superimposed to obtain the simulated long-crested waves, and the velocity and acceleration components in each direction of the waves were obtained according to the obtained harmonic function. Finally, the heave and pitch force/moment of the waves on the AUV were obtained by integration.

The theoretical research of waves shows that irregular waves can be decomposed into a large number of uniform and small regular waves. In studying the motion of AUV in irregular waves, the disturbing force/moment of waves can be studied by linear superposition method. By the knowledge of fluid mechanics we know that, the wave equation of plane waves on a point $(x, y, 0)$ in the earth-fixed coordinate system $o-xyz$ is

$$\eta_{\mathrm{w}}=\alpha_{\mathrm{w}}\cos(\omega_{\mathrm{w}}t-k_x x-k_y y) \tag{6}$$

where α_{w} is the wave amplitude; ω_{w} is the angular frequency of wave; $k_x=k_{\mathrm{w}}\cos\psi_{\mathrm{w}}$, $k_y=k_{\mathrm{w}}\sin\psi_{\mathrm{w}}$, where k_{w} is the wavenumber, and ψ_{w} is the wave angle.

When AUV sails near the water surface, the wave period described above is not equal to the wave period that AUV encounters during sailing. The wave period that AUV encounters during sailing is called the encounter period. In the calculation of AUV motion, the angular frequency of waves should be replaced by the angular frequency of encounter. The relation between the angular frequency ω_e of encounter and the angular frequency ω_w of waves is

$$\omega_e = \omega_w - \frac{k_w U_w}{g}\cos(\beta_w) \quad (7)$$

where U_w is the resultant velocity of the waves; g is gravitational acceleration; β_w is the encounter angle.

It is generally assumed that long-crested waves are linearly superposed by many regular waves of different crests and wavelengths. The initial phase θ_j is a random variable between 0–2π, and the mathematical expression of irregular long-crested waves is obtained.

$$\eta_w(x, y, t) = \sum_j^N \alpha_{wj}\cos(\omega_{wj}t - k_{xj}x - k_{yj}y + \theta_j), \quad j = 1, 2, \cdots, N \quad (8)$$

where α_{wj} is the amplitude of the j^{th} harmonic.

The spectrum recommended by the 11st International Towing Tank Conference (ITTC) in 1966 was adopted, which is generally called ITTC single parameter spectrum, and its expression is as follows:

$$S(\omega_w) = \frac{8.1\times10^{-3}\cdot g^2}{\omega_w^5}\exp(-\frac{3.11}{h_{1/3}\omega_w^4}) \quad (9)$$

where $h_{1/3}$ is the significant wave height of waves.

The amplitude of each harmonic can be obtained by the following formula:

$$\alpha_w = 2\sqrt{S(\omega_w)\mathrm{d}\omega_w} \quad (10)$$

In the coordinate system of waves, the velocity components of long-crested wave harmonics are as follows:

$$u_{wj} = \frac{2\pi\alpha_j}{T_j}\exp(-k_j z)^*\cos(\omega_{wj}t - k_{xj}x - k_{yj}y + \theta_j) \quad (11)$$

$$w_{wj} = \frac{2\pi\alpha_j}{T_j}\exp(-k_j z)^*\sin(\omega_{wj}t - k_{xj}x - k_{yj}y + \theta_j) \quad (12)$$

The acceleration components are as follows:

$$\dot{u}_{wj} = \frac{4\pi^2\alpha_j}{T_j^2}\exp(-k_j z)^*\sin(\omega_{wj}t - k_{xj}x - k_{yj}y + \theta_j) \quad (13)$$

$$\dot{w}_{wj} = -\frac{4\pi^2\alpha_j}{T_j^2}\exp(-k_j z)^*\cos(\omega_{wj}t - k_{xj}x - k_{yj}y + \theta_j) \quad (14)$$

In Formulas (11)–(14): u_{wj}, $\dot{u}_{wj}$ are respectively the velocity and acceleration components of wave harmonic in the wave propagation direction; w_{wj}, $\dot{w}_{wj}$ are respectively the velocity and acceleration components of wave harmonic in the vertical direction of sea level.

According to the superposition theorem and coordinate transformation, the total velocity component and acceleration component in the earth-fixed coordinate system $o-xyz$ can be obtained.

Total velocity components are:

$$[u_w]_E = \left[\sum_N u_{wj}\right]\cos(\psi_w) \quad (15)$$

$$[v_w]_E = \left[\sum_N u_{wj}\right]\sin(\psi_w) \quad (16)$$

$$[w_w]_E = \left[\sum_N w_{wj}\right] \quad (17)$$

Total acceleration components are:

$$[\dot{u}_w]_E = \left[\sum_N \dot{u}_{wj}\right]\cos(\psi_w) \quad (18)$$

$$[\dot{v}_w]_E = \left[\sum_N \dot{u}_{wj}\right]\sin(\psi_w) \quad (19)$$

$$[\dot{w}_w]_E = \left[\sum_N \dot{w}_{wj}\right] \quad (20)$$

In Formulas (15)–(20): $[u_w]_E$, $[\dot{u}_w]_E$ are velocity and acceleration components on the x axis respectively; $[v_w]_E$, $[\dot{v}_w]_E$ are velocity and acceleration components on the y axis respectively; $[w_w]_E$, $[\dot{w}_w]_E$ are velocity and acceleration components on the z axis.

Since the diameter of AUV is relatively small compared with the wavelength of waves, AUV can be considered as a slender cylinder. Moreover, the wave force acting on the AUV is caused by the distributary of fluid flowing around the AUV, not because of the diffraction force of the waves. From this we can see that the total wave force of AUV when sailing near the water surface can be obtained by using Morison equation, shown as follows:

$$F_{wx} = \left[\frac{C_d}{2}\rho A U_w^2 + C_m \nabla \rho \dot{U}_w\right]\mathrm{d}x \quad (21)$$

where C_d is drag coefficient; C_m is added mass coefficient; ρ is seawater density; A is projection area; ∇ is displacement; $\dot{U}_w$ is resultant acceleration of waves. By applying Sarpkaya's idea of wave force, and considering the operating environment of Dolphin MK II semi-submersible AUV, C_d and C_m are respectively 0.65 and 1.95.

Using the Morison equation for integration along the longitudinal direction of the ship, the heave force Z_{wave} and pitch moment M_{wave} of the waves near the water surface on the small AUV can be obtained respectively:

$$Z_{\text{wave}}=\int_L\left(C_{\text{d}}\frac{\rho D_0}{2}\left(w_{\text{w}}-w_j\right)^2+C_{\text{m}}\frac{\rho\pi D_0^2}{4}\left(\dot{w}_{\text{w}}-\dot{w}_j\right)\right)\mathrm{d}x \tag{22}$$

$$M_{\text{wave}}=\int_L\left(C_{\text{d}}\frac{\rho D_0}{2}\left(w_{\text{w}}-w_j\right)^2+C_{\text{m}}\frac{\rho\pi D_0^2}{4}\left(\dot{w}_{\text{w}}-\dot{w}_j\right)\right)x\mathrm{d}x \tag{23}$$

where D_0 is the diameter; w_{w} and $\dot{w}_{\text{w}}$ are respectively the heave velocity and acceleration of waves in the ship-fixed coordinate; w_j, $\dot{w}_j$ are respectively the velocity and acceleration components of AUV along the longitudinal direction of the ship coordinates $[u_{\text{w}}]_{\text{E}}$, $[v_{\text{w}}]_{\text{E}}$ and $[w_{\text{w}}]_{\text{E}}$ can be transformed to the ship-fixed coordinate system by using coordinate transformations:

$$\begin{bmatrix}u_{\text{w}}\\v_{\text{w}}\\w_{\text{w}}\end{bmatrix}_{\text{B}}=\underline{\boldsymbol{Q}}^{-1}\begin{bmatrix}u_{\text{w}}\\v_{\text{w}}\\w_{\text{w}}\end{bmatrix}_{\text{E}} \tag{24}$$

where $\underline{\boldsymbol{Q}}$ is the coordinate transformation matrix.

w and $\dot{w}$ in Formulas (22) and (23) can be obtained by using the following formulas:

$$w_j=w-qx_j \tag{25}$$

$$\dot{w}_j=\dot{w}-\dot{q}x_j-uq+vp \tag{26}$$

where w and $\dot{w}$ are the heave velocity and acceleration of AUV, respectively; q and $\dot{q}$ are angular velocity and acceleration of pitch, respectively; u is surge velocity; v is yaw velocity; x_j is the coordinate in the ship-fixed coordinate system.

3 Controller design

3.1 Linearization of the AUV dynamic model

In the study of motion control system of ship, because the ship motion is under control, it is considered that the ship has small amplitude motion near the equilibrium position under the effect of disturbances, and the ship motion can be linearized near the equilibrium position.

Unlike the surface motion body, AUV not only moves horizontally in sea level, but also has to perform heave motion in navigable depths. The 6-DOF motion of AUV can be divided into horizontal motion and vertical motion. In this paper, only the vertical motion of AUV is considered. The parameters of vertical motion are $\{u, w, q, \theta, z\}$, ignoring the horizontal motion, i.e. $v=p=r=\phi=0$. Ignoring the quadratic terms of w and q, we can get the simplified equation of AUV vertical motion:

$$\begin{bmatrix}m-Z_{\dot{w}} & -Z_{\dot{q}} & 0 & 0\\-M_{\dot{w}} & I_{yy}-M_{\dot{q}} & 0 & 0\\0 & 0 & 1 & 0\\0 & 0 & 0 & 1\end{bmatrix}\begin{bmatrix}\dot{w}\\\dot{q}\\\dot{z}\\\dot{\theta}\end{bmatrix}=$$
$$\begin{bmatrix}Z_w & (m-X_{\dot{u}})u_0+Z_q & 0 & 0\\(X_{\dot{u}}-Z_{\dot{w}})u_0+M_w & -Z_{\dot{q}}u_0+M_q & 0 & z_{\text{b}}B\\1 & 0 & 0 & -u_0\\0 & 1 & 0 & 0\end{bmatrix}\begin{bmatrix}w\\q\\z\\\theta\end{bmatrix}+$$
$$\begin{bmatrix}Z_{\delta_{\text{b}}} & Z_{\delta_{\text{s}}}\\M_{\delta_{\text{b}}} & M_{\delta_{\text{s}}}\\0 & 0\\0 & 0\end{bmatrix}\begin{bmatrix}\delta_{\text{b}}\\\delta_{\text{s}}\end{bmatrix}+\begin{bmatrix}Z_{\text{wave}}\\M_{\text{wave}}\\0\\0\end{bmatrix} \tag{27}$$

where m is the mass of AUV mass; u_0 is the velocity of AUV; $Z_{\dot{w}}$, $Z_{\dot{q}}$, Z_w, Z_q are the hydrodynamic force derivatives of the heave force; $X_{\dot{u}}$ is the hydrodynamic force derivative of surging force; $M_{\dot{w}}$, $M_{\dot{q}}$, M_w, M_q are hydrodynamic force derivatives of pitch moment; I_{yy} is the moment of inertia of AUV; z_{b} is the coordinate for the center of buoyancy; B is buoyancy; $Z_{\delta_{\text{b}}}$, $Z_{\delta_{\text{s}}}$ are the hydrodynamic force derivatives of heave force of the control surface; $M_{\delta_{\text{b}}}$, $M_{\delta_{\text{s}}}$ are the hydrodynamic force derivatives of pitch moment of control surface; δ_{b} is rudder angle of fore control surface; δ_{s} is rudder angle of aft control surface; $\dot{z}$ is vertical velocity; $\dot{\theta}$ is angular velocity of pitch in the earth-fixed coordinate system; θ is pitch angle; z is vertical displacement.

3.2 Controller

Linear Quadratic Regulator (LQR) refers to the system whose state equation is linear, and performance index is the quadratic function of the state variables and the control variables. Optimal control is one of the most important and typical optimization synthesis problems in the combined theory of linear systems. The characteristic of the optimization synthesis problem is that the control law of the system is derived by taking the maximum or minimum of the specified performance index function.

The state equation of the dynamic system is set as

$$\dot{\boldsymbol{x}}(t)=\boldsymbol{A}(t)\boldsymbol{x}(t)+\boldsymbol{B}(t)\boldsymbol{u}(t)$$
$$\boldsymbol{y}(t)=\boldsymbol{C}(t)\boldsymbol{x}(t) \tag{28}$$

where $\boldsymbol{x}(t)$ is n-dimensional state vector; $\boldsymbol{u}(t)$ is m-dimensional control vector; $\boldsymbol{y}(t)$ is l-dimensional output vector; $\boldsymbol{A}(t), \boldsymbol{B}(t), \boldsymbol{C}(t)$ are time-varying coefficient matrices. It is assumed that the error vector $\boldsymbol{e}(t)$ is

$$\boldsymbol{e}(t)=\boldsymbol{z}(t)-\boldsymbol{y}(t) \tag{29}$$

where $\boldsymbol{z}(t)$ is the l-dimensional expected output vector. The goal of the LQR controller is to find the optimal control vector $\boldsymbol{u}(t)$ so that any given initial state $\boldsymbol{x}(t_0)=\boldsymbol{x}_0$ can be shifted to the free end state $\boldsymbol{x}(t_f)$, and the performance index function has minimum values. Performance index is presented in the following form:

$$J(u)=\frac{1}{2}\boldsymbol{e}(t_f)^{\mathrm{T}}\boldsymbol{P}(t_f)\boldsymbol{e}(t_f)+\frac{1}{2}\int_0^T\left(\boldsymbol{e}(t)^{\mathrm{T}}\boldsymbol{Q}(t)\boldsymbol{e}(t)+\boldsymbol{u}(t)^{\mathrm{T}}\boldsymbol{R}(t)\boldsymbol{u}(t)\right)\mathrm{d}t \tag{30}$$

where $\boldsymbol{P}(t_f)$ is $l\times l$ symmetric positive semidefinite constant matrix; $\boldsymbol{Q}(t)$ is $l\times l$ weighting matrix for corresponding state variables, which is a symmetric positive semidefinite matrix; $\boldsymbol{R}(t)$ is $m\times m$ weighting matrix for corresponding control vectors, which is a symmetric positive definite matrix. Because $\boldsymbol{R}(t)$ is positive definite, when $\boldsymbol{u}(t)\neq 0$, $\boldsymbol{u}(t)^{\mathrm{T}}\boldsymbol{R}(t)\boldsymbol{u}(t)>0$. Because $\boldsymbol{Q}(t)$ is positive semidefinite, when $\boldsymbol{e}(t)\neq 0$, $\boldsymbol{e}(t)^{\mathrm{T}}\boldsymbol{Q}(t)\boldsymbol{e}(t)\geqslant 0$.

For the state adjustment problem, the performance index is in the following form:

$$J(u)=\frac{1}{2}\boldsymbol{x}^{\mathrm{T}}(t_f)\boldsymbol{P}(t_f)\boldsymbol{x}(t_f)+\frac{1}{2}\int_0^{\mathrm{T}}\left(\boldsymbol{x}^{\mathrm{T}}(t)\boldsymbol{Q}(t)\boldsymbol{x}(t)+\boldsymbol{u}^{\mathrm{T}}(t)\boldsymbol{R}(t)\boldsymbol{u}(t)\right)\mathrm{d}t \tag{31}$$

Using the minimum principle to solve the above problems, it is necessary to introduce Lagrange multipliers expressed by $\boldsymbol{\lambda}(t)$, which can form Hamiltonian function:

$$H(\lambda,x,u,t)=\frac{1}{2}\left[\boldsymbol{x}^{\mathrm{T}}(t)\boldsymbol{Q}(t)\boldsymbol{x}(t)+\boldsymbol{u}^{\mathrm{T}}(t)\boldsymbol{R}(t)\boldsymbol{u}(t)\right]+\boldsymbol{\lambda}^{\mathrm{T}}(t)\left[\boldsymbol{A}(t)\boldsymbol{x}(t)+\boldsymbol{B}(t)\boldsymbol{u}(t)\right] \tag{32}$$

To achieve the minimum performance index J, the optimal solution must satisfy the following conditions:

1) Canonical equations:

State equation

$$\dot{\boldsymbol{x}}(t)=\frac{\partial}{\partial\lambda}H(\lambda,x,u,t)=\boldsymbol{A}(t)\boldsymbol{x}(t)+\boldsymbol{B}(t)\boldsymbol{u}(t) \tag{33}$$

Co-state equation

$$\dot{\boldsymbol{\lambda}}(t)=-\frac{\partial}{\partial x}H(\lambda,x,u,t)=-\boldsymbol{Q}(t)\boldsymbol{x}(t)-\boldsymbol{A}^{\mathrm{T}}(t)\boldsymbol{u}(t) \tag{34}$$

2) Control equation:

$$\frac{\partial}{\partial u}H(\lambda,x,u,t)=\boldsymbol{R}(t)\boldsymbol{u}(t)+\boldsymbol{B}^{\mathrm{T}}(t)\boldsymbol{\lambda}(t)=0 \tag{35}$$

Namely,

$$\boldsymbol{u}^*(t)=-\boldsymbol{R}^{-1}(t)\boldsymbol{B}^{\mathrm{T}}(t)\boldsymbol{\lambda}(t) \tag{36}$$

3) Initial state:

$$\boldsymbol{x}(t_0)=\boldsymbol{x}_0 \tag{37}$$

4) Transversal condition:

$$\boldsymbol{\lambda}(t_f)=\frac{\partial}{\partial\boldsymbol{x}(t_f)}\left(\frac{1}{2}\boldsymbol{x}(t_f)^{\mathrm{T}}\boldsymbol{F}\boldsymbol{x}(t_f)\right)=\boldsymbol{F}\boldsymbol{x}(t_f) \tag{38}$$

where $\boldsymbol{F}$ is the terminal weighting matrix of the symmetric positive semidefinite constant.

In order to solve the above equations, we need to know $\boldsymbol{\lambda}(t)$. The LQR problem deals with the linear problem, so we can have the following hypothesis:

$$\boldsymbol{\lambda}(t)=\boldsymbol{P}(t)\boldsymbol{x}(t) \tag{39}$$

We can obtain that:

$$\dot{\boldsymbol{x}}(t)=\boldsymbol{A}(t)\boldsymbol{x}(t)-\boldsymbol{B}(t)\boldsymbol{R}^{-1}(t)\boldsymbol{B}^{\mathrm{T}}(t)\boldsymbol{P}(t)\boldsymbol{x}(t) \tag{40}$$

$$\dot{\boldsymbol{\lambda}}(t)=\dot{\boldsymbol{P}}(t)\boldsymbol{x}(t)+\boldsymbol{P}(t)\dot{\boldsymbol{x}}(t)=-\boldsymbol{Q}(t)\boldsymbol{x}(t)-\boldsymbol{A}(t)^{\mathrm{T}}\boldsymbol{P}(t)\boldsymbol{x}(t) \tag{41}$$

And the following optimal feedback control can be obtained:

$$\boldsymbol{u}(t)=-\boldsymbol{R}^{-1}(t)\boldsymbol{B}^{\mathrm{T}}(t)\boldsymbol{P}(t)\boldsymbol{x}(t)=-\boldsymbol{K}(t)\boldsymbol{x}(t) \tag{42}$$

where $\boldsymbol{K}(t)$ is feedback gain.

The structure of optimal feedback control system is shown in Fig. 2.

Riccati Equation is the first order nonlinear differential equations, and the numerical solutions are generally calculated by computer. $\boldsymbol{P}(t)$ can be obtained by the Riccati Equation. According to the finite time control law, the infinite time control law can be obtained as follows:

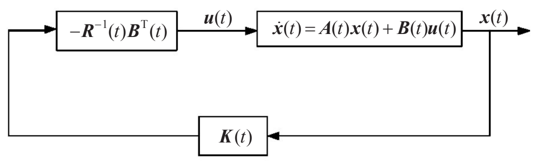

Fig.2 Structure of optimal feedback control system

Riccati Equation:

$$\boldsymbol{PA}+\boldsymbol{A}^{\mathrm{T}}\boldsymbol{P}-\boldsymbol{PBR}^{-1}\boldsymbol{B}^{\mathrm{T}}\boldsymbol{P}+\boldsymbol{Q}=0 \tag{43}$$

Optimal control:

$$\boldsymbol{u}^*=-\boldsymbol{R}^{-1}\boldsymbol{B}^{\mathrm{T}}\boldsymbol{Px}(t)=-\boldsymbol{Kx}(t) \tag{44}$$

Optimum performance index:

$$\boldsymbol{J}^*=0.5\boldsymbol{x}_0^{\mathrm{T}}\boldsymbol{Px}_0 \tag{45}$$

4 Drag force model

A coordinate system as shown in Fig. 3 was established, which includes the earth-fixed coordinate system $o-xyz$ and the ship-fixed coordinate system $o'-x'y'z'$. The earth-fixed coordinate system is fixed, and the ship-fixed coordinate system moves with the ship. The 6-DOF motion is u,v,w,p,q,r with the positive directions shown by the arrows in the figure. It is assumed that the initial state is that oo' overlaps, axes ox,oy,oz respectively overlap with axes ox',oy',oz', and the force on AUV in the earth-fixed coordinate system in the ox direction is F_{d}, namely, the sailing resistance; the force on AUV in the ship-fixed coordinate system in the $o'x'$ direction is $F_x^{'}$, force in the $o'y'$ direction is $F_y^{'}$ and that in the $o'z'$ direction is $F_z^{'}$. It is supposed that the AUV moves at the constant velocity of V in the direction the same as that of the ox, accompanied by small amplitude pitch motion in the plane of $x'o'z'$. Then $o'x'$ and ox are no longer in the same direction, with a pitch angle of θ between them. Velocity V and pitch velocity u of the AUV are no longer the same, with a pitch angle of θ between them. The pitch motion is a small amplitude motion, so we can consider $u \approx V$ numerically. Because it is a small amplitude pitch motion, according to the Taylor decomposition, it can be considered that $\sin\theta \approx \theta$, $\cos\theta \approx 1$, and the sailing resistance is

$$F_{\mathrm{d}} = F_x^{'} \cdot \cos\theta - F_y^{'} \cdot \sin\theta$$

That is

$$F_{\mathrm{d}} = F_x^{'} - F_y^{'} \cdot \theta \tag{46}$$

The pitch motion not only produces a pitch angle, but also affects $F_x^{'}$ and $F_z^{'}$. When AUV moves in water, its hydrodynamic force can be analyzed by potential flow theory. In an ideal infinite fluid, added resistance caused by AUV's pitch motion can be considered to be produced by the radiation potential of a submerged body, and the hydrodynamic force (i.e. $F_x^{'}, F_y^{'}, F_z^{'}$ in the ship-fixed coordinate system) on the AUV is

$$\boldsymbol{F} = \iint_{s_b(t)} \boldsymbol{p}\boldsymbol{n}\mathrm{d}s \tag{47}$$

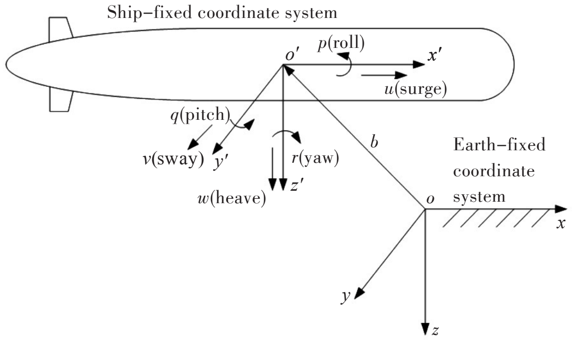

Fig.3 The earth-fixed coordinate and the ship-fixed coordinate

where $s_b(t)$ is the surface of the object; $\boldsymbol{n}$ is the unit normal vector of the surface, pointing to the interior of the object; $\boldsymbol{p}$ is the dynamic pressure, which is determined by Bernouli Equation, and its expression is as follows:

$$\boldsymbol{p} = -\rho\left(\frac{\partial \boldsymbol{\Phi}}{\partial t} + \frac{1}{2}\nabla\boldsymbol{\Phi} \cdot \nabla\boldsymbol{\Phi}\right) \tag{48}$$

where $\boldsymbol{\Phi}$ is the radiation velocity potential of the submerged body in the motion. Formula (48) is substituted into Formula (47), and based on inference, we can get

$$\boldsymbol{F} = -\rho\frac{\mathrm{d}}{\mathrm{d}t}\iint_{s_b(t)} \boldsymbol{\Phi}\boldsymbol{n}\mathrm{d}s \tag{49}$$

Considering the general case of AUV in 6-DOF non-stationary motion, $\boldsymbol{u}(t)$ is used to represent the translational velocity, $\boldsymbol{\omega}(t)$ is the rotational angular velocity around a center point moving with the body, thus the velocity potential on the surface should conform to the following boundary condition, i.e.

$$\frac{\partial \boldsymbol{\Phi}}{\partial \boldsymbol{n}} = \boldsymbol{u} \cdot \boldsymbol{n} + (\boldsymbol{\omega} \times \boldsymbol{r}') \cdot \boldsymbol{n} \tag{50}$$

where $\boldsymbol{r}'$ is the position vector starting from the center of rotation; the components of $\boldsymbol{u}$ and $\boldsymbol{\omega}$ in the ship-fixed coordinate system are denoted as $\boldsymbol{u} = (u_1, u_2, u_3)$ and $\boldsymbol{\omega} = (u_4, u_5, u_6)$.

Corresponding to the physical quantities in the ship-fixed coordinate system, there are $u_1 = u$, $u_2 = v$, $u_3 = w$, $u_4 = p$, $u_5 = q$, $u_6 = r$. Components $\boldsymbol{n}$ and $\boldsymbol{r}' \times \boldsymbol{n}$ are expressed as: $\boldsymbol{n} = (n_1, n_2, n_3)$, $\boldsymbol{r}' \times \boldsymbol{n} = (n_4, n_5, n_6)$.

Then the boundary condition Formula (50) can be rewritten as

$$\frac{\partial \boldsymbol{\Phi}}{\partial \boldsymbol{n}} = \sum_{i=1}^{6} u_i n_i \tag{51}$$

And we can get

$$\boldsymbol{F} = -\rho\sum_{i=1}^{6}\frac{\mathrm{d}}{\mathrm{d}x}[u_i(t)\iint_{s_b(t)} \boldsymbol{\Phi}_i(x_1^{'}, x_2^{'}, x_3^{'})\boldsymbol{n}]\mathrm{d}s \tag{52}$$

Formula (52) can be rewritten as

$$\boldsymbol{F} = -\rho\sum_{i=1}^{6}\dot{u}_i(t)\iint_{s_b}\boldsymbol{n}\mathrm{d}s - \rho\sum_{i=1}^{6}u_i(t)\boldsymbol{\omega} \times \iint_{s_b}\boldsymbol{\Phi}_i\boldsymbol{n}\mathrm{d}s \tag{53}$$

When AUV is in surge motion and pitch motion, considering variables $u_1, u_6(\omega_3)$ only, forces in the directions of $o^{'}x^{'}$ and $o^{'}z^{'}$ are isolated, and we get

$$\begin{aligned} F_x^{'} &= -m_{21}u_1u_6 - m_{26}u_6^2 \\ F_z^{'} &= -m_{11}u_1u_6 - m_{16}u_6^2 \end{aligned} \tag{54}$$

where m_{21}, m_{26}, m_{11}, m_{16} are hydrodynamic coefficients.

Taking into account the viscous damping force, $F_x^{'}$ is inversely proportional to $u_1^{\,2}$, and $F_z^{'}$ is proportional to the pitch angle, then $F_x^{'}$ and $F_z^{'}$ are corrected as

$$\begin{aligned} F_x^{''} &= -m_{21}u_1u_6 - m_{26}u_6^2 + m_{77}u_1^2 \\ F_z^{''} &= -m_{11}u_1u_6 - m_{16}u_6^2 + m_{88}\theta \end{aligned} \tag{55}$$

where m_{77} is the longitudinal force coefficient of u_1^2, and m_{88} is the vertical force coefficient of pitch angle θ.

Formula (55) is substituted into Formula (46). The negative sign refers to that direction of resistance is opposite to the ox positive direction. The negative sign is removed from the formula and we can obtain

$$F_{\mathrm{d}}=Au_6^2-B\theta u_6+C\theta^2+Du_1^2 \tag{56}$$

where $u_1=u\approx V, u_6=q$, so Formula (56) can be rewritten as

$$F_{\mathrm{d}}=Aq^2+B\theta q+C\theta^2+DV^2 \tag{57}$$

The above formula is the drag force model of AUV. A, B, C and D are undetermined coefficients. CFD simulation results of the AUV sailing resistance from a certain pitch period were selected, and undetermined coefficients can be obtained by using the linear regression method.

AUV can only bring limited energy when navigates underwater. In order to improve the endurance of AUV, it is necessary to control the energy consumption of AUV. When an AUV sails near the water surface, the disturbance of the waves leads to the attitude changes, and the sailing resistance increases because of the change of the vertical attitude, which leads to the increase of the energy consumption. In order to maintain the vertical attitude of the AUV, it is necessary to deflect a certain angle for the fore and aft control surfaces of the AUV, and the rotation of the fore and aft control surfaces will cause an increase in resistance. In order to minimize the AUV sailing resistance, the two factors are taken into account to obtain the optimal control.

The relation between added resistance by pitch and pitch was obtained in the above sections. The index function of energy saving can be converted to the following equation:

$$J=\frac{1}{t}\int_0^t(\lambda_1q^2+\lambda_2q\theta+\lambda_3\theta^2+\lambda_4u_1^2+\lambda_5u_2^2)\mathrm{d}t \tag{58}$$

where $\lambda_i(i=1,2,\cdots,5)$ is the value of minimum energy consumption index. The above formula is discretized, and considering the actual demand in this paper, the performance evaluation formula of the sailing resistance and energy consumption can be expressed as

$$J=\frac{1}{N}\sum_{i=1}^{N}\left(\lambda_1q^2+\lambda_2q\theta+\lambda_3\theta^2+\lambda_4u_1^2+\lambda_5u_2^2\right) \tag{59}$$

5 Simulation results

Firstly, the performance index of energy consumption was established; then, LQR controller was designed with this performance index, and the wave disturbance was added; finally, a Simulink simulation model was built to carry out simulation analysis and test for the control effect of LQR controller. The simulation conditions are as follows: the sea state is 3, the significant wave height is 0.88 m, the average period is 6.43 s, and $C_{\mathrm{m}}=1.95$. It was simulated when the AUV sails at a velocity of 4.5 m/s at the depth of $d=3$ m under the wave heave force and pitch moment of the encounter angle β_{w} of 45°, as shown in Fig. 4 and Fig. 5. The simulation curves of the disturbing force/moment vs. pitch displacement and pitch angle response of the AUV vertical motion without control and under LQR control are shown in Fig. 6 and Fig. 7.

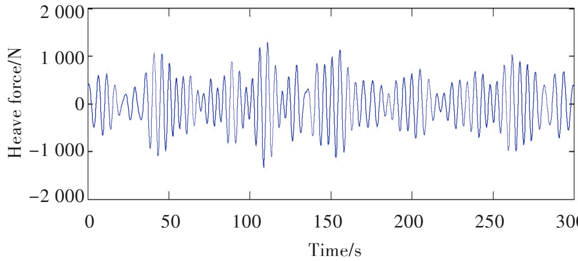

Fig. 4 Result of heave force when $\beta_{\mathrm{w}}=45°$, $d=3$ m

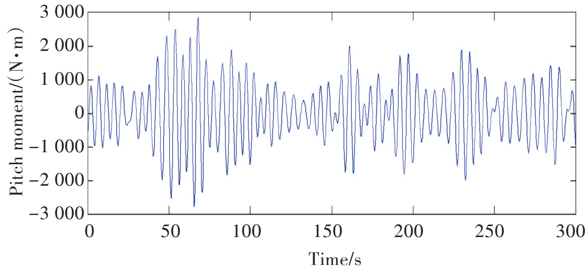

Fig. 5 Result of pitch moment when $\beta_{\mathrm{w}}=45°$, $d=3$ m

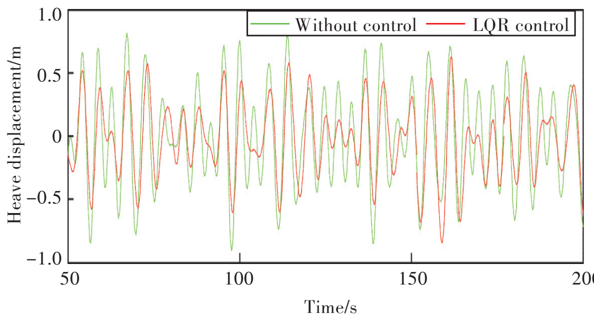

Fig.6 Time histories of the heave displacement of AUV

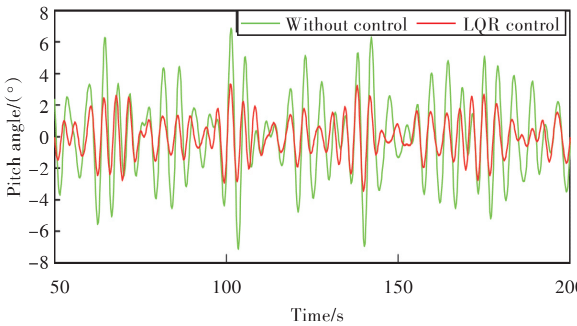

Fig.7 Time histories of the pitch angle of AUV

From the simulation curves in Fig. 6 and Fig. 7, it can be seen that the designed LQR controller of AUV vertical motion can effectively suppress the vertical attitude motion of AUV, and has good control effect. After LQR control was added, the heave displacement decreased from the previous maximum amplitude of 0.981 2 m to 0.619 6 m, with a decrease amplitude of 36.85%. The pitch angle was reduced from the previous maximum value of 6.83° to 3.02°, with a decrease amplitude of 55.77%. The designed LQR controller can effectively cancel the disturbances of waves, and the maximum amplitude of pitch angle and heave displacement both obviously reduced. Therefore, when the LQR controller was added to the AUV vertical motion, the motion became stable, the sailing resistance became smaller, and the energy consumption was reduced.

The angle amplitude of the fore and aft control surfaces of the AUV was limited to 15°, and the deflection angles of the fore and aft control surfaces are shown in Fig. 8 and Fig. 9.

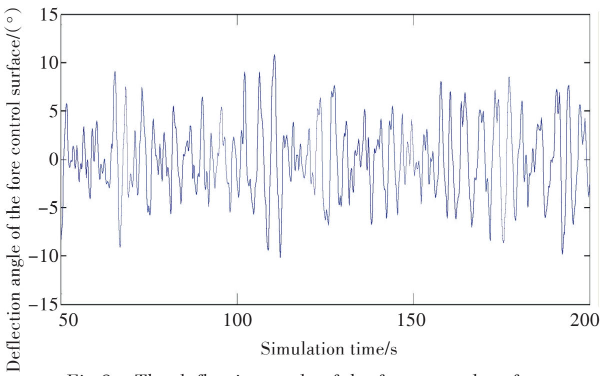

Fig.8 The deflection angle of the fore control surface with LQR control

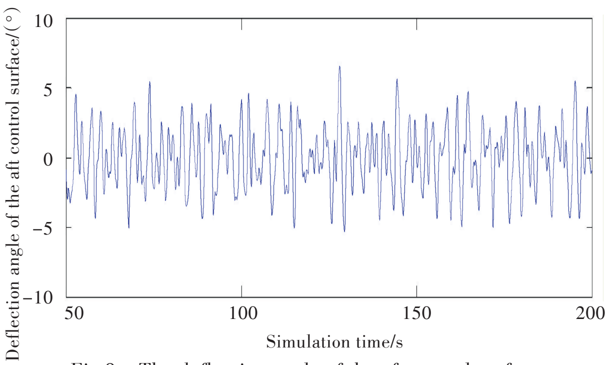

Fig.9 The deflection angle of the aft control surface with LQR control

In this paper, variance was used to evaluate the control effect, and the formula of pitch stabilization effect is defined as follows:

$$E=(V_{\mathrm{a}}-V_{\mathrm{b}})/V_{\mathrm{a}}*100\% \tag{60}$$

where E is the pitch stabilization effect; V_{a} is the variance of pitch angle/heave displacement before the stabilization; V_{b} is the variance of pitch angle/heave displacement after the stabilization.

The standard of heave stabilization was defined in the same way. Control results were analyzed statistically, and the results are shown in Table 2.

Table 2 Effect statistics of attitude control

	Without control	LQR control
Maximum value of heave/m	0.981 2	0.709 7
Maximum value of pitch angle/(°)	6.831 3	3.301 0
Heave displacement variance/m^2	0.148 6	0.079 3
Pitch angle variance/(°)^2	6.858 5	1.534 8
Effect of heave stabilization/%	–	46.64
Effect of pitch stabilization/%	–	77.62

It can be seen from Table 2 that the vertical attitude control effect of AUV is good, and the heave displacement and pitch angle were effectively reduced by adding LQR control. By the definition of attitude control criterion (Formula (60)), it can be seen that the LQR control made the effects of heave and pitch stabilization for AUV reach 46.64% and 77.62% respectively.

The added resistance before and after control is shown in Fig. 10 and Fig. 11.

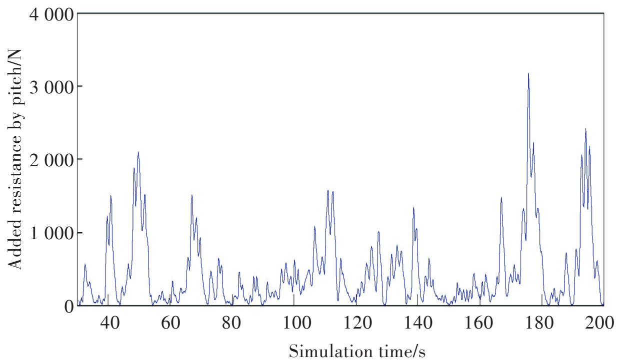

Fig.10 Added resistance without control

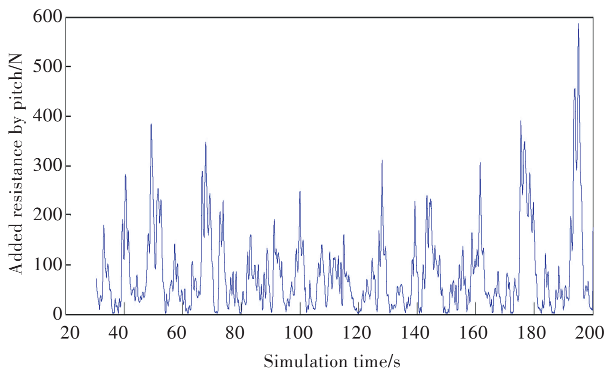

Fig.11 Added resistance with LQR control

As shown in Fig. 10, Fig. 11 and Table 3, after adding LQR control, the added resistance of the AUV by pitch was reduced effectively, the energy consumption of the AUV propeller was reduced, and the optimal control of the AUV attitude and energy was realized.

6 Conclusion

In this paper, a mathematical model between the

Table 3　Effect statistics of added resistance control

	Without control	LQR control
Mean added resistance/N	437.039 2	81.153 5
Standard deviation of added resistance/N	488.747 5	82.154 8

sailing resistance and the sailing attitude was established, and the drag force model was defined as the performance index of LQR. On this basis, the weighting matrix of LQR controller was determined and the LQR controller was designed. The effect of heave and pitch stabilization by LQR control method was up to 46.64% and 77.62% respectively. Meanwhile, the added value of the sailing resistance was reduced to 1/6 of the original value, achieving satisfactory control results.

In controlling the AUV sailing attitude near the water surface, the pitch stabilization and the reduction of the sailing resistance can be optimized simultaneously to reduce the energy consumption of AUV. In this paper, we proposed to use the AUV model of the sailing resistance as the performance index of LQR controller, and achieved satisfactory results, which can provide a new control idea for the energy consumption reduction and the sailing resistance reduction of AUV.

References

[1] Intersessional Meeting of the Greenhouse Gas Working Group. Progress report on the work relating to fw coefficient in the energy efficiency design index (EEDI) [C]//The 59th Session of the Marine Environmental Protection Committee. London UK: IMO, 2009.

[2] JIN H Z, WANG F. Driving models and optimal control for fin stabilizers at zero speed[J]. Journal of Huazhong University of Science and Technology (Natural Science Edition), 2010, 38(3): 66-68 (in Chinese).

[3] LIU Z Q, JIN H Z. Extended radiated energy method and its application to a ship roll stabilisation control system[J]. Ocean Engineering, 2013, 72: 25-30.

[4] EVANS J, NAHON M. Dynamics modeling and performance evaluation of an autonomous underwater vehicle [J]. Ocean Engineering, 2004, 31 (14/15): 1835-1858.

[5] OSTAFICHUK P M. AUV hydrodynamic and modelling for improved control [D]. Vancouver, Canada: University of British Columbia, 2004.

[6] DING T J. Design of control law for longitudinal multi-degrees of freedom variable stability based on LQR[J]. Flight Dynamics, 2016, 34(3): 86-89 (in Chinese).

[7] LI Y B, CHEN C, ZHANG X L. Research on control algorithm for flying wing UAV based on improved LQR technology [J]. Control Engineering of China, 2014, 21(5): 628-633 (in Chinese).

[8] DUAN Z. Robust servo LQR flight control law design of UAV[J]. Computer Measurement & Control, 2015, 23(8): 2713-2715 (in Chinese).

[9] BHUSHAN R, CHATTERJEE K, SHANKAR R. Comparison between GA-based LQR and conventional LQR control method of DFIG wind energy system[C]// Proceedings of the 3rd International Conference on Recent Advances in Information Technology (RAIT). Dhanbad, India: RAIT, 2016: 214-219.

[10] HÄUSLER A J, SACCON A, AGUIAR A P, et al. Energy-optimal motion planning for multiple robotic vehicles with collision avoidance[J]. IEEE Transactions on Control Systems Technology, 2016, 24(3): 867-883.

[11] LIANG X, HUA X J, SU L F, et al. Energy conservation control strategy of autonomous underwater vehicle for ocean search[J]. Journal of Coastal Research, 2015, 73: 589-593.

[12] PETRICH J, STILWELL D J. Model simplification for AUV pitch-axis control design[J]. Ocean Engineering, 2010, 37(7): 638-651.

[13] WANG H J, WANG L L, PAN L X. Research on roll stabilizing based on energy optimization for autonomous surface vehicle[J]. Journal of Applied Mathematics, 2014, 2014: 347589.

[14] XU J A, REN L G, YANG L P, et al. Generalized predictive control and energy consumption analysis of autonomous underwater vehicle[J]. Control Theory & Applications, 2009, 26(10): 1148-1150(in Chinese).

[15] CHYBA M, HABERKORN T, SINGH S B, et al. Increasing underwater vehicle autonomy by reducing energy consumption[J]. Ocean Engineering, 2009, 36 (1): 62-73.

[16] SARKAR M, NANDY S, VADALI S R K, et al. Modelling and simulation of a robust energy efficient AUV controller[J]. Mathematics and Computers in Simulation, 2016, 121: 34-47.

[17] LI J, HUANG D B, DENG R. Numerical calculation and model tests for drag and power prediction of a manned submersible[J]. Journal of Harbin Engineering University, 2009, 30(7): 735-740 (in Chinese).

[*Continued on page* 91]

2012, 2(3): 148-157.
[16] IM W S, WANG C, TAN L, et al. Cooperative controls for pulsed power load accommodation in a shipboard power system[J]. IEEE Transactions on Power Systems, 2016, 31(6): 5181-5189.
[17] TROVÃO J P, MACHADO F, PEREIRINHA P G. Hybrid electric excursion ships power supply system based on a multiple energy storage system[J]. IET Electrical Systems in Transportation, 2016, 6(3): 190-201.
[18] SEENUMANI G, SUN J, PENG H. A hierarchical optimal control strategy for power management of hybrid power systems in all electric ships applications[C]// Proceedings of the 49th IEEE Conference on Decision and Control. Atlanta, GA: IEEE, 2010: 3972-3977.
[19] KIM S Y, CHOE S, KO S, et al. A naval integrated power system with a battery energy storage system: fuel efficiency, reliability, and quality of power[J]. IEEE Electrification Magazine, 2015, 3(2): 22-33.
[20] SKJONG E, SUUL J A, RYGG A, et al. System-wide harmonic mitigation in a diesel-electric ship by model predictive control[J]. IEEE Transactions on Industrial Electronics, 2016, 63(7): 4008-4019.
[21] KIM S Y, CHOE S, KO S, et al. Electric propulsion naval ships with energy storage modules through AFE converters[J]. Journal of Power Electronics, 2014, 14(2): 402-412.

柴电混合电力推进船舶负载频率 H_∞ 鲁棒控制

李洪跃, 王锡淮, 肖健梅, 陈晨
上海海事大学 物流工程学院,上海 201306

摘　要:[**目的**]风、浪及海流等多种随机不确定因素会引起船舶综合电力系统负载频率的波动。[**方法**]采用电池补偿柴油发电机组输出功率与船舶需求功率之间的差值,对柴油发电机组进行二次调频控制,保证船舶电网功率平衡,抑制电网频率波动。建立综合电力推进系统频率控制状态空间模型,基于 H_∞ 混合灵敏度原理,选取合理的灵敏度与补灵敏加权函数设计鲁棒控制器,采用线性矩阵不等式(LMI)方法对设计的控制器进行求解并进行算例仿真。[**结果**]系统幅频特性表明,设计的鲁棒控制器具有合理性,短时冲击信号作用下的性能表现满足指标要求。与传统PI控制器的对比结果表明,设计的鲁棒控制器能显著抑制随机扰动引起的电网负载频率波动,减小柴油发电机组与电池的功率变化,电池荷电状态(SOC)变化范围明显缩小,可提高船舶电力系统鲁棒稳定性与鲁棒性能。[**结论**]该系统在各种工况下都能稳定运行并且使电网频率稳定,同时提高柴油发电机组燃油经济性,减小废气排放。

关键词: 混合电力推进; 负载频率控制; 线性矩阵不等式; 混合灵敏度; H_∞ 鲁棒控制

[*Continued from page* 82]

基于航行阻力优化的近水面机器人减纵摇控制

姚绪梁, 孟令卫, 牛小丽
哈尔滨工程大学 自动化学院,黑龙江 哈尔滨 150001

摘　要:[**目的**]水下机器人(AUV)在近水面航行时,不可避免地会受到海浪的干扰,海浪干扰导致的纵摇和升沉运动不仅会影响AUV的航行姿态,同时也会导致其航行阻力增加,加剧能源的消耗。为实现AUV航行姿态和航行阻力的加权最优,[**方法**]建立AUV的六自由度模型并进行纵平面运动的线性化。对AUV的纵摇增阻情况进行研究,利用势流理论的方法,推导AUV的纵摇增阻模型。以纵摇增阻为性能指标,确定控制器中的 $\boldsymbol{Q}$ 矩阵和 $\boldsymbol{R}$ 矩阵,并设计减小AUV纵摇的线性二次型控制系统(LQR)控制器。[**结果**]仿真结果表明,加入LQR控制器后,减垂荡和减纵摇效果分别达到46.64%和77.62%,纵摇增阻减小到原来的1/6。[**结论**]研究结果显示,基于能量优化的LQR控制可实现纵摇增阻和航行姿态的加权最优,节约能量消耗,增加AUV的续航力。

关键词: 航行阻力优化; LQR控制; 纵摇减摇; 势流理论